The stress-induced protein NUPR1 orchestrates protein translation during ER-stress by interacting with eIF2α

Maria Teresa Borrello[1], Patricia Santofimia-Castaño[1], Marco Bocchio[2], Angela Listi[1], Nicholas Fraunhoffer[1], Christopher Pin[1,3], Philippe Soubeyran[1], Eric Chevet[4] and Juan Iovanna[1]

[1] Centre de Recherche en Cancérologie de Marseille, INSERM U1068, CNRS UMR 7258, Aix-Marseille Université and Institut Paoli-Calmettes, Parc Scientifique et Technologique de Luminy, 13288 Marseille, France;

[2] INMED (INSERM U1249), Aix-Marseille University, Turing Center for Living Systems, Parc Scientifique de Luminy, 13273, Marseille, France;

[3] Departments of Pediatrics, Oncology, and Physiology and Pharmacology, Schulich School of Medicine, University of Western Ontario Children's Health Research Institute, London, ON, Canada N5C 2V5;

[4] INSERM U1242, Proteostasis and Cancer Team, Chemistry Oncogenesis Stress Signaling, Université de Rennes 1, Rennes, France

Corresponding author address: Juan Iovanna, email: juan.iovanna@inserm.fr. Centre de Recherche en Cancérologie de Marseille (CRCM), INSERM U1068, CNRS UMR 7258, Aix-Marseille Université and Institut Paoli-Calmettes, Parc Scientifique et Technologique de Luminy, 163 Avenue de Luminy, 13288 Marseille, France. Phone +33-491828803; Mobil Phone +33-760988158; Fax +33-491 826083.

Abstract

NUPR1 is an 82 amino-acids protein overexpressed upon cell injury in virtually all organs including the exocrine pancreas. Despite NUPR1's well established role in the response to cell stress, the molecular and structural machineries triggered by NUPR1 activation remain largely unknown. Here we report that NUPR1 plays a central role during the endoplasmic reticulum stress response. Biochemical analysis revealed a general attenuation of the unfolded protein response in pancreas of mice lacking NUPR1. Ultrastructural analysis of pancreata revealed fewer morphological alteration in tunicamycin-treated *Nupr1*$^{-/-}$ compared to *Nupr1*$^{+/+}$. A bioinformatical analysis of potential interacting partners of NUPR1 showed significant enrichment in translation initiation factors, including eIF2α. Co-immunoprecipitation of tagged NUPR1 confirmed that the protein binds to both eIF2α and its phosphorylated form (p-eIF2α). Depletion of NUPR1 lead to prolonged phosphorylation of eIF2α. Finally, click chemistry revealed NUPR1-depleted Panc-1 cells displayed a decrease in the amount of nascent proteins in response to ER stress induction compared to wild-type cells. Thus, NUPR1 is necessary for an efficient PERK-branch activation by binding to the p-eIF2α and, consequently, promoting protein synthesis during the ER stress response.

Keywords: NUPR1, UPR, ER-stress, eIF2α, protein translation

Introduction

NUPR1, also known as p8 or Com1, is an intrinsically-disordered protein first identified during the onset of pancreatitis (1). Since its discovery, this 8 kDa protein has been extensively studied and we and others demonstrated that it is transiently induced in almost all organs in response to a variety of cell injuries (2–6), including minimal stresses such as the renewal of culture medium (7). Although NUPR1's distinct functions are still debated, it is clear that it acts as an essential element during the stress cell response, protecting cells from genotoxic or oxidative injury (Barbosa-Sampaio et al. 2013; Clark et al. 2008; Hamidi et al. 2012, Taieb 2005). The highest expression of NUPR1 has been reported in pancreatic acinar cells, which are highly enriched in endoplasmic reticulum (ER) and have the highest rate of protein synthesis among all organs (12, 13). The major function of the ER is to fold and perform post-translational modifications to secreted and integral membrane proteins. Also, it maintains the homeostasis between folded and unfolded proteins (14, 15) and disturbance of such physiological ER activities leads to a cell stress response implicated in a variety of pathological states (14, 16, 17). Several evidence indicates that NUPR1 is involved in the onset of the ER stress but its role in this context remains largely unexplored (18, 19).

ER stress, with its consequent accumulation of unfolded proteins in the ER, triggers several signaling pathways that, together, are termed the unfolded protein response (UPR). The ultimate goal of the UPR is to resolve homeostatic imbalance between folded and unfolded proteins. If a failure in restoring protein homeostasis occurs, the UPR triggers apoptosis to safely dispose of damaged cells. The UPR is comprised of three main branches: PKR-like ER kinase (PERK), inositol-required enzyme 1 (IRE1) and activation transcription factor 6 (ATF6). In the absence of stress, these molecules are bound to the chaperone BiP (GRP78). When excessive protein load occurs, BiP dissociates from PERK, IRE1 and ATF6, leading to their activation (21). Activation of the PERK branch leads to phosphorylation of the eukaryotic initiation factor 2α (eIF2α), which is a critical regulator of protein translation. Phosphorylated eIF2α prompts a dramatic reduction in protein translation to decrease cellular amino-acid consumption. However, some transcription factors, including ATF4, escape this translation block. Among other functions, ATF4 increases cell survival by promoting the expression of genes involved in protein folding, amino-acid import and biosynthesis of aminoacyl-transfer RNAs (Harding et al. 2003). When protein homeostasis is restored, GADD34/PPP1R15A dephosphorylates eIF2α to restore normal protein synthesis (Harding et al. 2003). Prolonged or excessive ER stress activation leads to programmed cell death, mainly mediated by the activation of the CCAAT/enhancer binding protein (C/EBP)

homologous protein (CHOP) (16, 24) which promotes apoptosis via the intrinsic mitochondrial pathway.

In the present work we report that NUPR1 constitute an important element of the UPR activation. By using several complementary approaches (*in vitro* and *in vivo* NUPR1 gain and loss of function) we shed light on the ER-stress-NUPR1 crosstalk and demonstrated that the cellular overexpression of NUPR1 serves to physically interact with eIF2α and phospho-eIF2α. Depletion of NUPR1 led in fact to an overtime extended phosphorylation of eIF2α and a consequent longer attenuation of global protein synthesis. On the contrary, in NUPR1-*WT* models we observed a faster restoration of normal protein translation. Ablation of NUPR1 showed an aberrant expression of the downstream genes of the PERK branch which expression is reported to be either delayed or significantly downregulated compared to the NUPR1-*WT* counterpart. Altogether, we identified NUPR1 as a novel binding partner for eIF2α and suggest a role for NUPR1 in the regulation of eIF2α mediated cellular stress response pathway.

Results

Biochemical evaluation of ER-stress activators in pancreatic acinar cells of *Nupr1*$^{+/+}$ and *Nupr1*$^{-/-}$ mice

Recently, we reported that the pancreatic transcriptomes of mice lacking *Nupr1* (*Nupr1*$^{-/-}$) showed a strong downregulation of mRNAs related to ER stress (18). This prompted us to hypothesize that NUPR1 is necessary for mediating a correct ER stress response. To test the importance of NUPR1 in the onset of the ER-stress response we induced a pharmacological activation of the UPR (single injection of Tunicamycin; Tun, 1.0 µg/g) in *Nupr1*$^{-/-}$ and *Nupr1*$^{+/+}$ mice. Tun induces ER stress by inhibiting protein *N*-Glycosylation, thereby preventing correct protein folding (25). After 16h, pancreata were extracted and biochemical analysis by western blot and RT-qPCR were performed in order to evaluate the expression levels of the major UPR mediators of the PERK and IRE1-α branches (Figure 1). The accumulation and activation (phosphorylated isoform) of PERK appeared to be similar between the two genotypes. Consistently with activation of PERK signaling, increased expression of ATF4 was observed in both *Nupr1*$^{-/-}$ and *Nupr1*$^{+/+}$ following activation of cell stress. However, the expression of ATF4 was reduced in *Nupr1*$^{-/-}$ mice at both protein and mRNA levels compared to *Nupr1*$^{+/+}$ counterpart following Tun injection ($p < 0.0001$). This suggested that NUPR1 could act downstream of PERK within the UPR. Reduced or altered ATF4 function was supported by a totally hampered expression of the protein CHOP in *Nupr1*$^{-/-}$ pancreata. While we observed reduced induction of CHOP mRNA expression in *Nupr1*$^{-/-}$ mice compared to *Nupr1*$^{+/+}$ after stress (effect of Tun: $p < 0.0001$; effect of genotype

$p < 0.0001$; interaction $p < 0.0001$; *Nupr1*$^{+/+}$ vs *Nupr1*$^{-/-}$ in Tun condition: $p < 0.0001$, *post hoc* Sidak test, n=9), an increase in CHOP mRNA was still observed suggesting protein translation may be affected.

The biochemical examination of the IRE1α branch activation showed that IRE1α and its p-IRE1α isoform were expressed without significant variation in both genotypes. However, western blot analysis showed that pancreatic expression of the chaperone BiP was almost halved in *Nupr1*$^{-/-}$ mice compared to *Nupr1*$^{+/+}$ mice (n=6). Consistently, expression of the mRNA coding for BiP showed to be downregulated in *Nupr1*$^{-/-}$ mice models compared to *Nupr1*$^{+/+}$ littermates (n=9). For both protein and mRNA, two-way ANOVA analysis revealed a significant effect of Tun ($p < 0.0001$ for protein expression and $p < 0.0010$ for mRNA). Subsequent corrected multiple comparisons uncovered a significant difference between *Nupr1*$^{+/+}$ and *Nupr1*$^{-/-}$ mice after Tun administration ($p < 0.0001$ for protein and $p = 0.0228$ for mRNA analysis, *post hoc* Sidak test) but not in control conditions.

BiP is a stress sensor of the UPR and an integral part of the ER quality control system. Upon UPR initiation, the translational efficiency of BiP is normally increased by two to three folds and regulated by several overlapping mechanisms (26). The downregulation of protein and mRNA expression could be therefore correlated with a faulty UPR machinery in *Nupr1*$^{-/-}$ mice, in accordance with previously reported *in vitro* and proteomic data (18). Similar levels of total IRE1α, p-IRE1α and spliced XBP1 (XBP1s) protein were observed in both *Nupr1*$^{+/+}$ and *Nupr1*$^{-/-}$ treated mice, suggesting that an effective activation of the IRE1α branch occurred. However, a significant difference was detected between the two genotypes when examining *Xbp1s* mRNA levels (Figure 1D). The increase in *Xbp1s* mRNA induced by stress in *Nupr1*$^{-/-}$ mice was significantly lower compared to *Nupr1*$^{+/+}$ mice (effect of Tun: $p < 0.0001$; effect of genotype $p = 0.0030$, with no interaction between the two factors; *Nupr1*$^{+/+}$ vs *Nupr1*$^{-/-}$ in Tun condition: $p < 0.0001$ *post hoc* Sidak test, n=9). To validate the decrease of *Xbp1s* in *Nupr1*$^{-/-}$ models, we evaluated the mRNA expression of *Erdj4, a* known target of XBP1s transcriptional regulation (27). Unsurprisingly, the gene resulted downregulated in *Nupr1*$^{-/-}$ mice compared to the *Nupr1*$^{+/+}$ littermates ($p = 0.001$). Taken together, the evidence presented here suggests the absence of NUPR1 leads to a general attenuation of the UPR after ER stress induction.

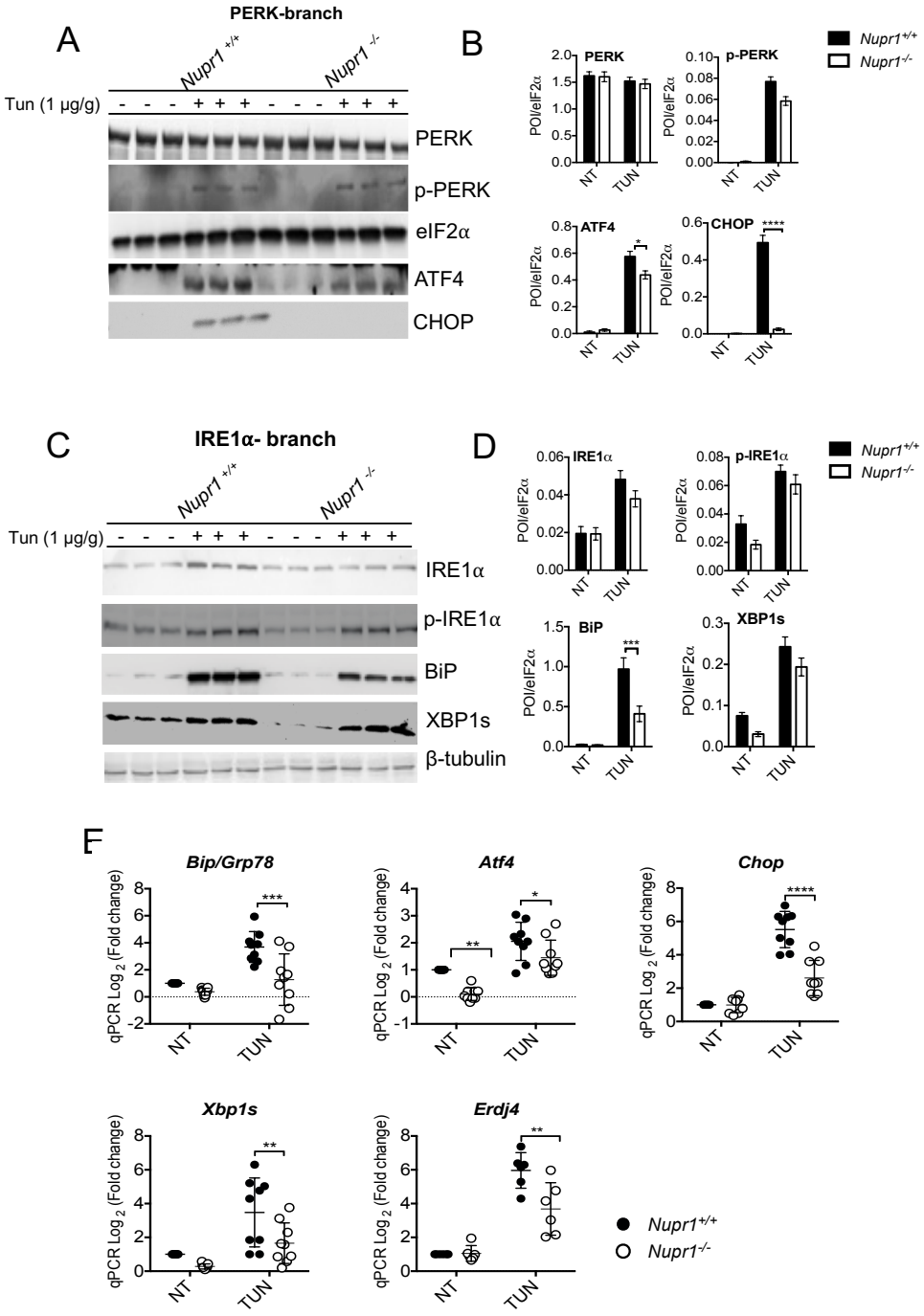

Figure 1 *Biochemical evaluation of ER-stress related proteins after Tunicamycin induction in Pancreas. Western blot analysis was performed to evaluate protein levels of major UPR activators of PERK branch (A) and its quantification (B) and IRE1α branch (C) and its quantification (D) in pancreatic extracts of Nupr1$^{+/+}$ Nupr1$^{-/-}$ mice. Quantification of protein of protein was performed by comparison to loading control. Data are means of triplicates ± SEM. Statistically significant differences between Nupr1$^{+/+}$ and Nupr1$^{-/-}$ mice are shown (*p < 0.02, **p < 0.01, ***p = 0.001, ****p<0.0001). D) RNA was extracted from Nupr1$^{+/+}$ and Nupr1$^{-/-}$ pancreata treated with 1 µg/g Tunicamycin or vehicle (NT), to evaluate the mRNA levels of the genes involved in ER stress response using RT-qPCR. Statistically significant differences are shown (*p < 0.03, **p < 0.001, ***p = 0.001, ****p < 0.0001).*

NUPR1-deficiency prevents ultrastructural alterations in murine pancreatic acinar cells after Tunicamycin-induced cell stress

Next, we studied the consequences of the lack of NUPR1 expression on ER stress induced ultrastructural modifications. To this end we injected Tun (1 µg/g) in both *Nupr1*$^{+/+}$ and *Nupr1*$^{-/-}$ mice and 16 h or 36 h post-treatment, we perfusion-fixed the mice to perform ultrastructural analysis of acinar cells using transmission electron microscopy. Representative micrographs are shown in Figure 2. In non-treated exocrine pancreatic cells (Figures 2A and 2B) the ER was structurally ordered into long, thin, densely packed *cisternae* covered with ribosomes for both genotypes (black arrows). Overall, cellular ultrastructure was normal: acinar cells showed a regular polarized organization with visible nuclei (mononucleated cells, Nu) with linear membrane, several electron dense zymogen granules (zy) and mitochondria with visible crests (mit). At 16 h post-injection, acinar cells in *Nupr1*$^{+/+}$ mice displayed dilated and expanded ER with nearly complete loss of associated ribosomes (Figure 2C) in the perinuclear area and fewer electron dense zymogen granules. Expanded ER *cisternae* are a cellular hallmark of the UPR. The ER membranes expand on their own to alleviate the stress due to an excessive load of misfolded proteins. With increased ER volume, the concentration of unfolded protein intermediates decreases. Thus, proteins gain more time to fold, leading to avoidance of aggregate formation (28). As time progressed, damage to the ER was more aggravated in *Nupr1*$^{+/+}$ mice, becoming fragmented with a visible impact on mitochondria morphology (Figure 2E). Such ER abnormalities were observed in *Nupr1*$^{+/+}$ samples in more than 40% of the analyzed acinar cells (12/30 cells from ten randomly selected fields of acquisition). Conversely, such ER dilation was almost absent in *Nupr1*$^{-/-}$ samples (Figure 2F). While a decrease in zymogen granules was also detected in *Nupr1*$^{-/-}$ pancreata (Figure 2D), even 36 h after Tun treatment, little to no expansion of the ER was observed. Altogether, these data show that in absence of NUPR1, activation of cellular stress leads to an altered restoration of protein homeostasis following induction of the UPR in pancreatic acinar cells.

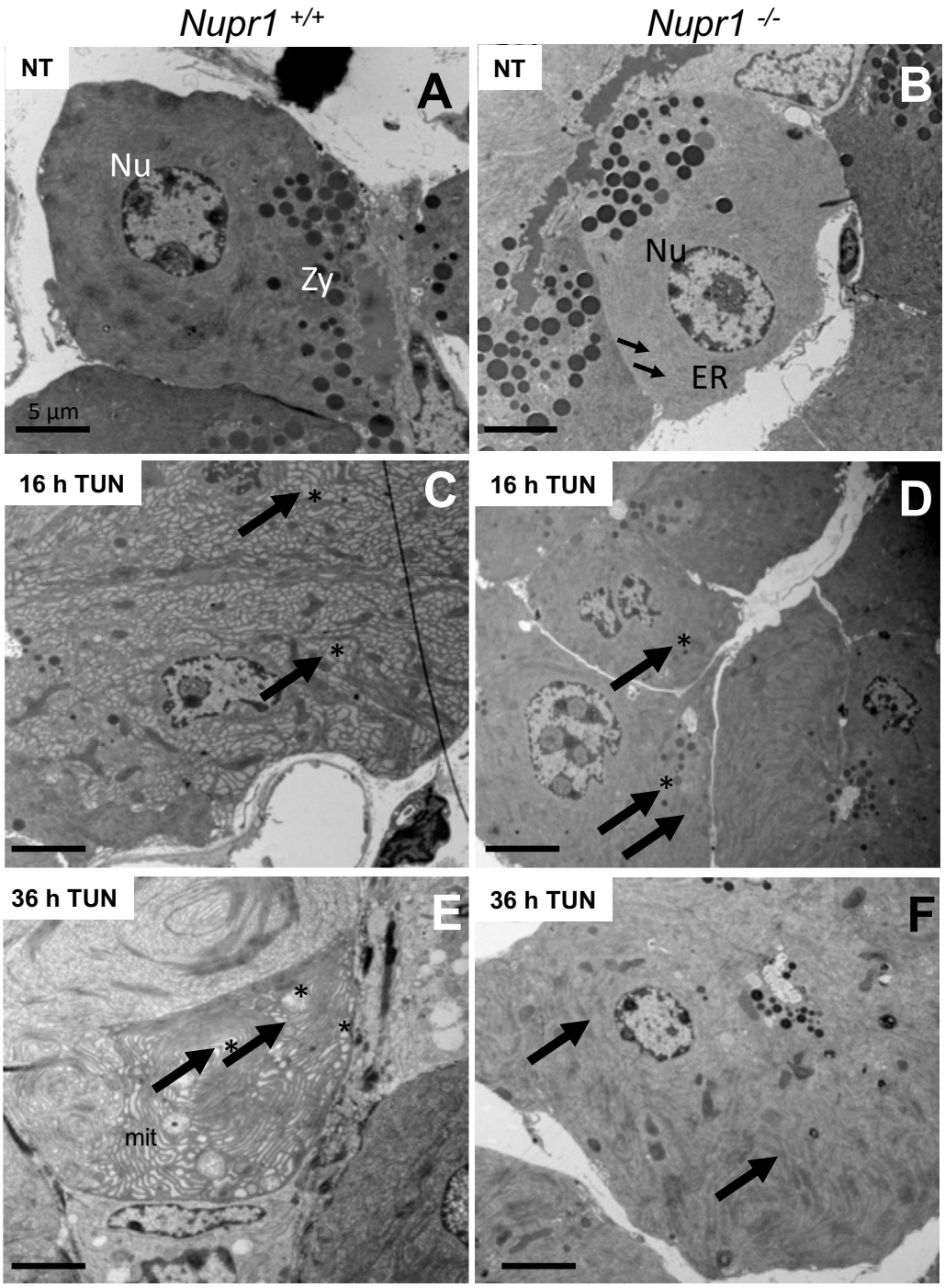

Figure 2: *Ultrastructure analysis of Nupr1$^{+/+}$ and Nupr1$^{-/-}$ murine pancreata after ER stress induction with Tunicamycin. Figure show representative pictures of perfusion fixed mice pancreata ultrathin sections from Nupr1+/+ and Nupr1-/- mice injected with vehicle (NT, A and B) or Tunicamycin (TUN, 1.0 µg/g),16 h (C and D) and 36 h (E and F) post injection. Arrows point to the ER (B); asterisk and arrow show dilated ER cisternae (C) in comparison to (D, KO) where the dilatation is not important. Abbreviation used: Nu = nucleus; zy = zymogen granules; Mit = mitochondria*

Identifying the role of NUPR1 during ER stress response

To understand the molecular mechanisms by which NUPR1 regulates the UPR, we next attempted to identify its molecular partners. To this end Flag-tagged NUPR1 was expressed in MiaPaCa-2 cells, then immunoprecipitated from cell lysates following 24 h ER-stress, induced by either glucose starvation or 1 μM Thapsigargin (TPS) treatment (Figure 3). NUPR1-associated proteins were identified by mass spectrometry. As a control, similar IP-mass spectrometry was performed under normal conditions. Mass-spectrometry results identified 656 NUPR1-interacting proteins under normal conditions (Supplementary Table 1), and 1152 or 828 interacting proteins under glucose-starvation (Supplementary Table 2) and TPS (Supplementary Table 3) conditions, respectively (Figure 3A). Five hundred and seventy seven proteins were common to all conditions, with 7, 365 and 77 proteins specific to control, glucose-starvation and TPS treatments, respectively (Figure 3A). Bioinformatic analysis using the String protein-protein interaction database showed significant enrichment in translation initiation factors. Twenty two of a total of 142 proteins directly involved in translation initiation were identified under unstressed conditions (p = 4.14e-07) suggesting NUPR1 is involved in protein translation regulation (Table 1). Most importantly, the number of NUPR1-interacting proteins increased to 73 (*p* = 5.19e-36) in glucose-starvation and 45 (*p* = 4.76e-21) in TPS-treated cells (Table 1). Therefore, the role of NUPR1 in translational regulation appears to be enhanced during ER stress. The NUPR1 interactome involved in translation included several translation initiation factors. This group of proteins was expanded under ER stress and included at least three eukaryotic initiation factor subunits, eIF2α (eIF2S1), eIF2β (eIF2S2), and eIF2γ (eIF2S3) (Figure 3B). Since eIF2α is phosphorylated by PERK during ER stress, it is important to determine if NUPR1's ability to interact with eIF2α was affected by its phosphorylation. Using co-immunoprecipitation for GFP-tagged NUPR1 (Figure 3C), we confirmed that NUPR1 could interact with both eIF2α and phosphorylated eIF2α (p-eIFα) in MiaPaCa-2 cells. The interaction between NUPR1 and eIF2α was increased by glucose starvation and, more dramatically, by TPS treatment, supporting the mass spectrometry data.

To further confirm the association between NUPR1 and p-eIF2α/eIF2α we performed proximity ligation assay (PLA, Duolink®), which identifies molecular complexes directly within the cells. PLA directly resolves the binding of proteins that occurs at distances smaller than 16 Å. Confocal fluorescent microscopy revealed PLA positive foci under all conditions, suggesting that NUPR1 interacts with eIF2α regardless of stress conditions. In addition, this interaction appears to be extranuclear, which would be expected for a direct interaction to eIF2α and p-eIF2α. PLA also revealed increased interaction following either TPS treatment and glucose starvation, with the formation of NUPR1-eIF2α and NUPR1-p-eIF2α complexes

remaining in the perinuclear area (Figure 4A and C). These observations confirm that NUPR1 interacts with eIF2α and p-eIF2α and ER stress increases these interactions. Combined, our data suggests a novel role for NUPR1 regulating the translational machinery during ER stress.

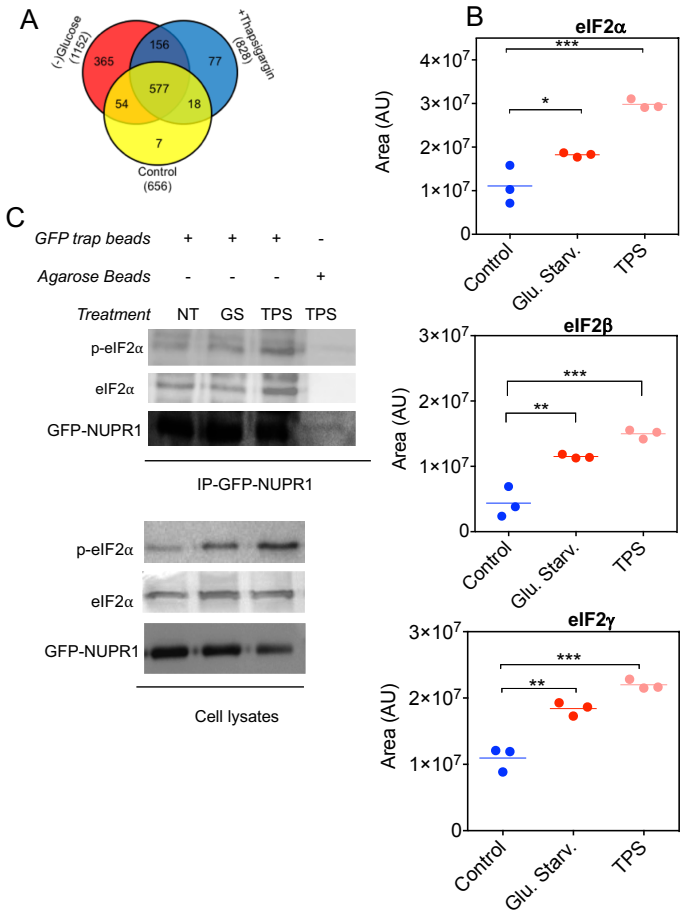

*Figure 3: Identification of NUPR1 partners in ER stress. A) Venn diagram showing NUPR1 associated proteins after glucose starvation or thapsigargin (TPS, 1 μM, 24h) treatment. B) Quantification of mass spectrometry peak areas of NUPR1-associated eukaryotic initiation factors (n=3, one-way ANOVA, *p = 0.02, **p = 0.002, ***p = 0.0002). C) Co-Immunoprecipitation assay of GFP-tagged-NUPR1 to detect the association of NUPR1 with p-eIF2α and eIF2α. GFP-NUPR1-transiently transfected MiaPaCa-2 cells extracts were subjected to co-immunoprecipitation with GFP-trap beads or Agarose beads followed by western blotting with the antibodies against p-eIF2α and eIF2α.*

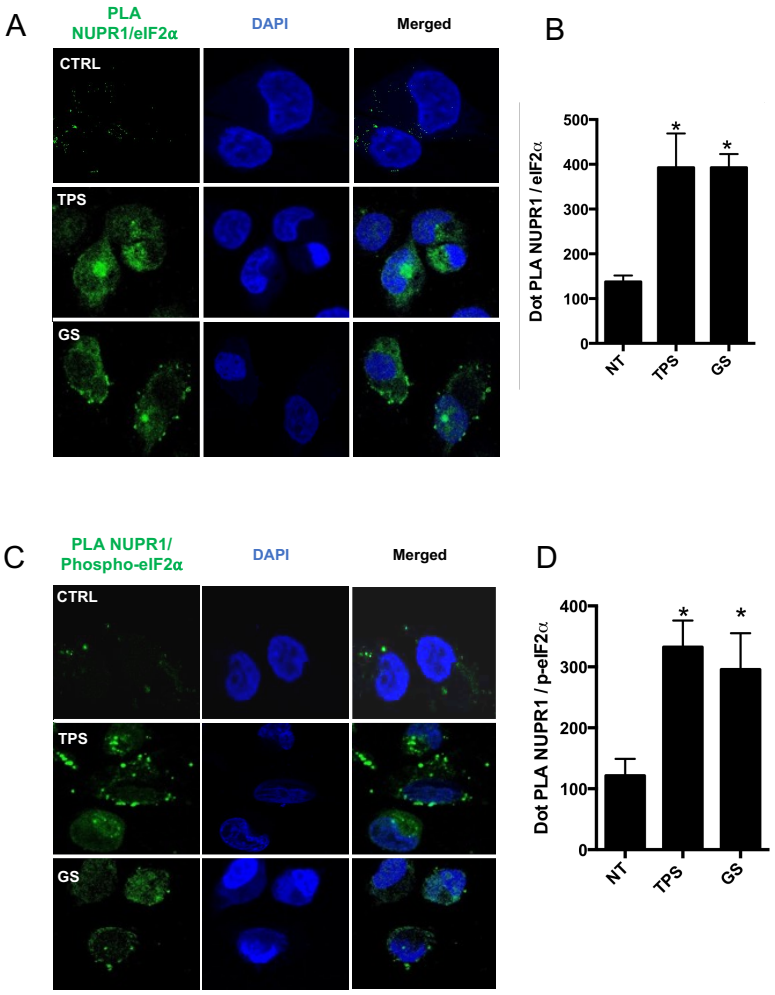

***Figure 4**. In situ PLA of eIF2α or p-eIF2α and Flag-NUPR1. Mouse anti-Flag and human and anti-eIF2α (A) and anti-p-eIF2α (C) respectively were used to reveal the interaction between the proteins in MiaPaCa-2 cells; cells were incubated with Thapsigargin (TPS, 1 μM, 24h) or Glucose starved (GS, 24 h). (B-D) PLA quantification was done by counting the number of green dots with ImageJ; data are means of 10 field each containing not less than 150 nuclei (*p ≤ 0.001). Magnification 60x.*

NUPR1-depletion enhances eIF2α phosphorylation and affects de-novo protein synthesis during stress

So far, our data suggests that NUPR1 interacts with p-eIF2α likely to alleviate stress and restore protein translation. In such a model, we would predict that loss of NUPR1 would increase p-eIF2α. To test this model, we studied the phosphorylation of eIF2α during the ER stress response in Panc-1 with (*NUPR1*$^{+/+}$) and without *NUPR1* (*NUPR1*$^{-/-}$ generated by Crispr/Cas9 deletion of NUPR1 as previously reported (29). Both cell lines were treated with 1 μM of TPS up to 9 h. As showed in Figure 5A, NUPR1-depleted cells showed higher levels of phosphorylated eIF2α compared to *WT* cells. The results prompt us to investigate whether the absence of NUPR1 interferes with expression of downstream effectors of eIF2α

signaling, specifically CHOP and GADD34 mRNAs. Surprisingly, RT-qPCR revealed reduced and deferred expression of both CHOP and GADD34 mRNAs at all time points (Figure 5B). Overall, the data showed that NUPR1 interfere with the phosphorylation of eIF2α and thereby its inhibition, resulting in a sustained expression of downstream target genes.

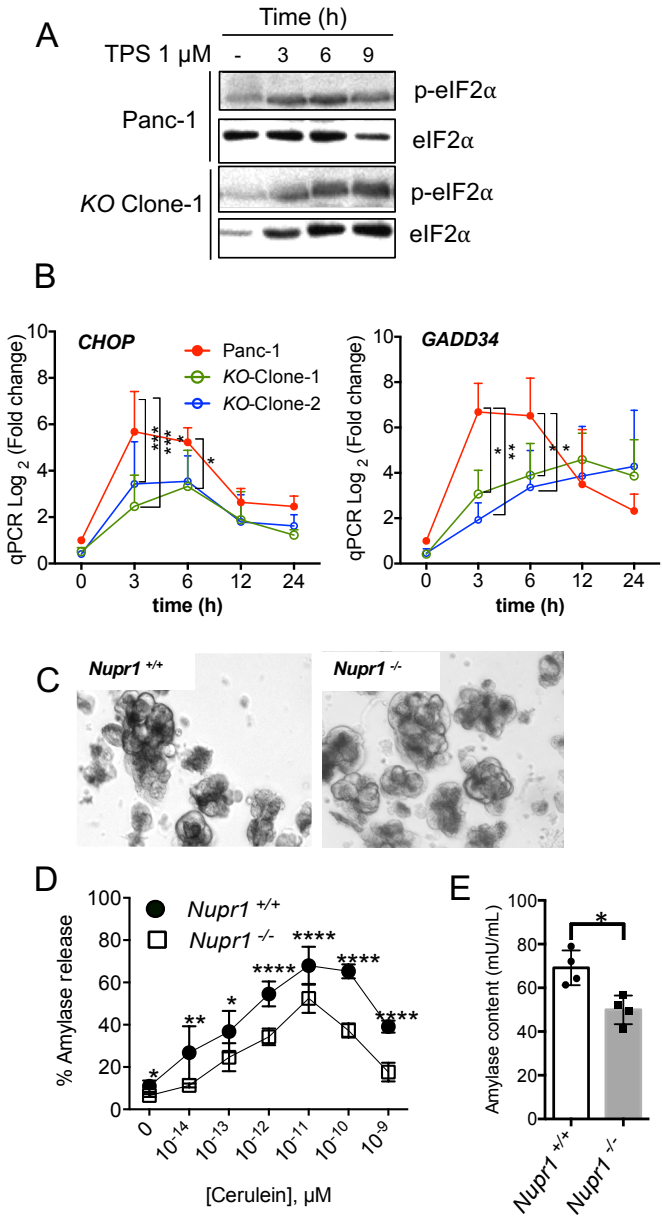

Figure 5. *EIF2α phosphorylation in NUPR1 deficient Panc-1 and matched control (Panc-1) in response to Thapsigargin induced ER-stress. A) The whole cell lysates were analysed by Western Blotting using phosphorylated eIF2α antibody. B) mRNA expression of CHOP and GADD34 genes in NUPR1 deficient cells and matched control cells was analyzed overtime by qPCR after 1 μM incubation with thapsigargin. Significant results are reported in the graph (****p < 0.0001, ***p<0.001, **p =0.0012, *p=0.04) NUPR1 expression affects de-novo protein synthesis during stress. Digested acinar cells from Nupr1$^{+/+}$ or Nupr1$^{-/-}$ murine pancreata; D) Amylase release curve of murine isolated acinar cells stimulated during 30 min with increasing concentration of Cerulein. Acinar cells released amylase in the medium in a dose-dependent manner from a basal level to a plateau in both*

*genotypes being the secretion in WT significantly higher ; statistical significance was determined with a two-way ANOVA and post hoc Sidak test (*p<0.01, **p<0.014, ****p < 0.0001, n = 4 mice and three technical replicate for experiment). E) Amylase total content in Nupr1$^{-/-}$ was significantly lower than from acini of Nupr1$^{+/+}$; statistical significance was determined with unpaired two-tailed t-test *p< 0.04, n = 4 mice per genotype and 3 technical replicates).*

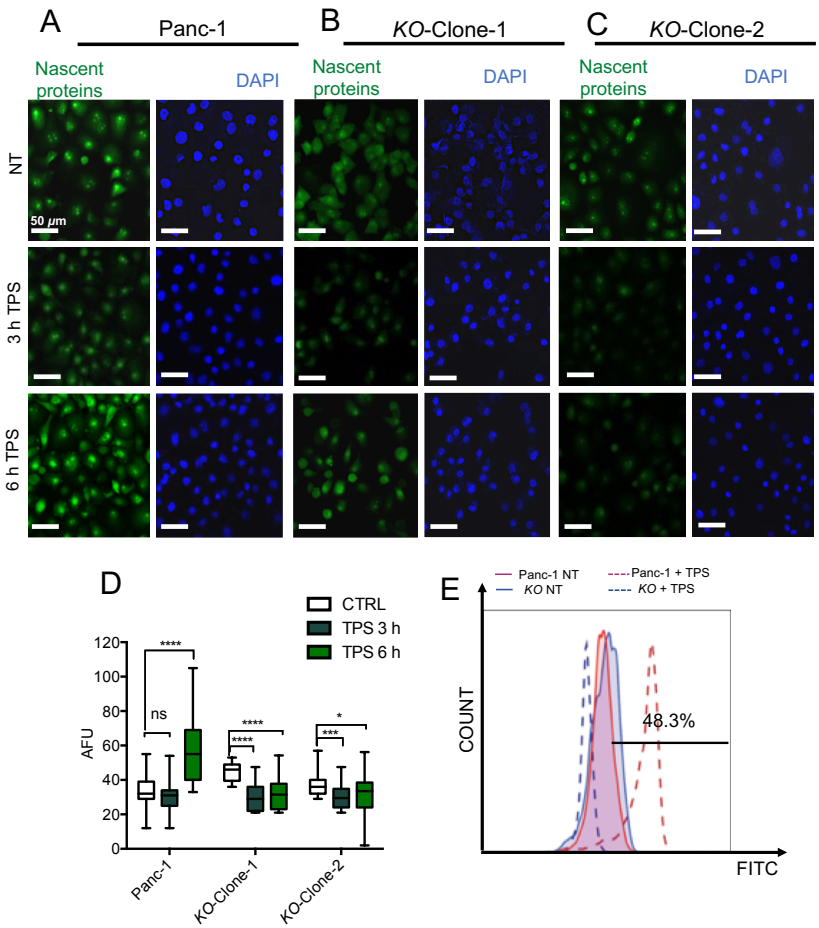

***Figure 6**. Imaging nascent proteins in pancreatic cultured cells with OP-puro. A) Cultured Panc-1 WT or Crisper/Cas9 edited for NUPR1 (KO-Clones 1 and 2, B and C) cells were incubated for 1h or 3h with 1 µM of TPS. The cells were subsequently incubated for 1h with OP-puromycin. PFA fixed cells were stained by CuAAC with FITC-azide, and imaged by Confocal microscopy. Arbitrary Fluorescent intensity (AFU) was measured with imageJ is reported in graph D. Two-way ANOVA with a post hoc Sidak test were used to determine statistical significance (**p = 0.001, ****p< 0.001). E) Flow cytometry of de-novo protein synthesis measured with OP-puromycin. Cells were gated based on forward scatter (FSC) and side scatter (SSC) parameters. In the X-axis are reported the mean fluorescence increase of WT or KO clone Panc-1 cells subjected to click chemistry of integrated OP-puromycin conjugated with FITC azide. In the Y-axis is reported the cell count.*

Restored protein synthesis is an important aspect of the UPR because it is thought to maintain the ER stress (16, 24, 30) but is also required for recovery of the cell. Since NUPR1 limits phosphorylation of eIF2α, we speculated it promotes sustained protein synthesis. To test this hypothesis, we measured secretion of amylase and the load content in *ex-vivo* pancreatic acini from *Nupr1*$^{+/+}$ and *Nupr1*$^{-/-}$ mice (Figure 5C). The analysis of amylase secretion following 30 min incubation with increasing concentrations of caerulein (a secretogogue analogue of cholecystokinin) (31) showed caerulein induced amylase release in a dose-dependent manner in both genotypes (Figure 5D, effect of caerulein: $p < 0.012$, two-way ANOVA). However, amylase secretion from *Nupr1*$^{-/-}$ acini was significantly lower than from *Nupr1*$^{+/+}$ acini (Figure 5D, effect of genotype: $p < 0.0001$, two-way ANOVA) while amylase content was higher in *Nupr1*$^{+/+}$ acini than in *Nupr1*$^{-/-}$ acini (all $p < 0.05$, *post hoc* Sidak test) (Figure 5E).

Next, we sought to evaluate NUPR1's ability to modulate the level of protein synthesis. To this end, the amount of nascent protein in *NUPR1*$^{+/+}$ and *NUPR1*$^{-/-}$ Panc-1 pancreatic cells was quantified with click chemistry label. Following 3h or 6h TPS treatment (1 μM; Figure 6), cells were incubated with a puromycin analogue bearing a propargyl group for 1 h, allowing co-translational incorporation at the C-terminus of nascent polypeptides chains. The incorporated propargyl-puromycin formed an *in-situ* covalent conjugate by copper catalyzed click reaction with a fluorescently labelled azide (FITC-azide). The reaction enables subsequent analysis of protein synthesis based on FITC fluorescence levels using confocal microscopy and cytometry. Three hours into TPS incubation, NUPR1$^{+/+}$ Panc-1 cells did not show changes in fluorescence, whereas NUPR1$^{-/-}$ cells displayed lower levels of fluorescence compared to untreated cells (Figure 5A-C and quantification D). This decreased fluorescence was confirmed by two-way ANOVA, which showed an effect of both TPS ($p < 0.0001$) and NUPR1 ($p < 0.0001$), as well as an interaction between the two factors ($p = 0.001$). Six hours into TPS incubation, *NUPR1*$^{+/+}$ Panc-1 cells showed increased fluorescence which is proportional with increased nascent protein production. Conversely, both *NUPR1*$^{-/-}$ clones maintained lower levels of fluorescence (Figure 5G). Two-way ANOVA analysis revealed no main effect of TPS ($p = 0.592$), but again an effect of NUPR1 ($p < 0.0001$) and an interaction between the two factors ($p < 0.0001$). Confocal results were confirmed at 6h of TPS treatment by flow cytometry (Figure 5D).

Discussion

Nupr1 is a stress-induced gene, rapidly activated in response to a variety of stresses, including several ER stress inductors such as serum starvation, cycloheximide, ceramide, staurosporine and CCl4 (2, 4, 6, 19, 32). Until now, NUPR1's roles within the UPR remained

unknown. In this study, we demonstrate NUPR1-deficient pancreatic cells are unable to activate a complete ER stress response indicating that NUPR1 is an essential factor for a complete UPR activation. While ATF4 and XBP1s are increased, their transcriptional targets are expressed at significantly lower levels in *Nupr1*$^{-/-}$ mice. Our results also strongly support a function for NUPR1 in re-establishing the translational machinery following induction of ER stress. First, NUPR1-deficient cells show reduced protein translation only following induction of stress. This is combined with a lack of ER dilation, typically associated with re-activation of general protein translation. Second, we show a direct interaction of NUPR1 with p-eIF2α using multiple methodologies. Co-IP and mass spectrometry indicate a direct interaction between NUPR1 and p-eIF2α, while PLA shows colocalization at perinuclear regions that increases upon stress. Finally, we show that while mRNA transcription for UPR-associated genes may increase, the accumulation of these proteins (specifically CHOP) does not, confirming a specific deficit in protein translation in the absence of NUPR1.

Mechanistically, we have demonstrated, by using several complementary approaches, that NUPR1 regulates translation during ER stress by associating with p-eIF2α/eIF2α and most probably negatively regulating p-eIF2α phosphorylation in order to restore normal protein synthesis. As a consequence, in NUPR1-deficient cells, protein synthesis is almost completely arrested throughout the prolonged phosphorylation of eIF2α and, consequently, its decreased activity, resulting in a lighter ER stress response. The UPR is an important intracellular signaling pathway that has evolved to maintain cellular homeostasis. It finely tunes responses to various stresses such as metabolic, oxidative or inflammatory conditions (33). Its maladaptive response has been implicated in a variety of diseases including metabolic disease, neurodegenerative disease, inflammatory disease, and cancer. The main goal of the acute activation of UPR is to restore the ER homeostasis (12, 30), by setting on simultaneous mechanisms directed to clean the ER from misfolded proteins. These mechanisms include ubiquitination followed by proteasome degradation of the misfolded proteins (34, 35), autophagy (16, 36), the transitory arrest of protein synthesis and RNA processing to stop the accumulation of the misfolded neo-proteins into the ER. When these mechanisms are efficient, the cell is destined to survive. Conversely, when these mechanisms are inadequate or sustained, the ER stressed cells start a programmed cell death (16).

Our data demonstrate that NUPR1 not only functions as a mediator of acute responses to the ER stress by its ability to prompt the induction of CHOP as demonstrated in our experiment, but overall by regulating the cellular decision and influencing the protein translation through its interaction with several factors involved directly in translation initiation

and regulation. Importantly, these interactions were promoted by ER stress inductors. An important point to be noted is that NUPR1 interacts with eIF2α as well as its phosphorylated form p-eIF2α suggesting that under stress conditions in which NUPR1 is activated, NUPR1 could play a translation-promoting role.

In conclusion, our findings demonstrate that NUPR1 plays a role against the protein neo-synthesis inhibition which occurs during ER stress to reach an equilibrium and favor cell survival. Collectively, our data support an essential role of NUPR1 during ER stress by acting against the phospho-dependent negative regulation of eIF2α.

Materials and methods

Study approval

All experimental protocols were carried out in accordance with the nationally approved guidelines for the treatment of laboratory animals. All experimental procedures on animals were approved by the Comité d'éthique de Marseille numéro 14 (C2EA-14) in accordance with the European Union regulations for animal experiments.

Mouse strains and Tissue collection.

For all the *in vivo* experiments we used *Nupr1*$^{-/-}$ mice bear a homozygous deletion of exon 2 (37). Mice were used between the 5 and 16 weeks of age and as control we used their mating littermates. Animals were kept in the Experimental Animal House of the Centre de Cancérologie de Marseille (CRCM) of Luminy. After sacrifice by cervical dislocation, pieces of pancreas were collected and frozen in cold isopentane for further analysis or directly homogenized in 4 M guanidium isothiocyanate lysis buffer for efficient pancreatic RNA extraction according with Chirgwin et al's procedure (38).

Tunicamycin injections

Mouse of 5-8 weeks of age were injected intraperitoneally with 1 µg/g of Tunicamycin (Sigma) using 150 mM of D-Glucose as vehicle. After 16 h post-injection mice were sacrificed and organs collected.

Cell culture

MiaPaCa-2 and Panc-1 cells were purchased from ATCC and cultures in DMEM medium (Dulbecco's modified Eagle's medium, Gibco, Life Technologies, Carlsbad, CA, USA),

supplemented with 10% fetal bovine serum (Lonza, Basel, Switzerland) and cultured at 37ºC and 5% CO_2. Cells were used in all experiments below 20 passages.

Preparation or protein lysates and Western Blotting

Forty mg of frozen tissue were cut on dry ice and homogenized with Precellys® (Bertin instruments) in 300 µL of ice-cold Rippa buffer (10 mM Tris-Cl (pH 8.0), 1 mM EDTA, 0.5 mM EDTA, 1% Triton X-100, 0.1% sodium deoxycholate, 0.1% SDS, 140 mM NaCl), complemented with 0.5 µg/g of protease inhibitor kit (Sigma), 200 µM of Na_3VO_4, 1 mM of PMSF and 40 mM of β-glycerophosphate. After homogenization, the supernatant was cleared by centrifugation for 30 min at 14.000 rpm at 4°C. Protein lysate content was quantified by micro BCA assay (Thermo-Fisher Scientific) and 40 µg of protein were resolved by SDS-PAGE, transferred to nitrocellulose membrane for 1 or 2 h. Membranes were next blocked with TBS (tris-buffered saline) in 5% BSA and blotted overnight with primary antibody (1:500 dilution in TBS 5% BSA). After washes, the membrane was incubated with HPR-conjugated secondary antibody (Boster, Pleasanton CA, USA) for 1 h at room temperature (1:5000 dilution in TBS-5% BSA). Subsequently, the membrane was washed and revealed with ECL (enhanced chemo-luminescence). Chemiluminescent signal was detected in a G-Box (Syngene). The following antibodies were used: rabbit monoclonal ATF4 (D4B8), mouse monoclonal CHOP (L63F7), rabbit monoclonal XBP1s (E9V3E), rabbit monoclonal, BiP (C50B12), rabbit monoclonal eIF2α XP® (D7D3), rabbit monoclonal Phospho-eIF2α XP® (Ser51) (D9G8), and rabbit monoclonal Phospho-PERK (Thr980) were from Cell Signaling Technology; (G.305.4), rabbit polyclonal antibody Phospho-IRE1 alpha (Ser724) (PA1-16927) is from Thermo Fisher; and mouse monoclonal β-actin (#A5316) is from Sigma.

Preparation of RNA and RT-qPCR

RNA from murine pancreata was extracted after 16 h of intraperitoneal injections of Tunicamycin following the Chirgwin procedure (38). Total RNA from cells was obtained using RNAeasy kit (Quiagen) following manufacturer's instruction. The RNA integrity was assessed with Agilent 2100 Bioanalyzer with the RNA 6000 Nano chip Kit. The RNAs were reverse-transcribed using GO Script kit (Promega) following manufacturer's instruction. RT-qPCR were performed using Aria mix using Promega reagents. Primer sequences are available upon request.

Transmission Electron Microscopy

Mice were perfused with 4% cold PFA and 2.5% glutaraldehyde. Pancreatic tissue was then immersed overnight in 0.1M Soresen buffer, post-fixed in 1% osmium tetroxide, and in bloc

stained with 3% uranyl acetate. The tissue was dehydrated with increasing concentrations of ethanol on ice and acetone before being embedded in Epon. Ultrathin sections (70 nm) were prepared using a Leica UCT Ultramicrotome (Leica, Austria) and stained with uranyl acetate and lead citrate and deposited on formvar-coated slot grids. The grids were observed in an FEI Tecnai G2 at 200 KeV and acquisition was performed on a Veleta camera (Olympus, Japan).

NUPR1 expression vector transfection

MiaPaCa-2 cells were seeded in 12-well plates and transfected with 3 µg of DNA (NUPR1-GFP, NUPR1-Flag or control vector) and 3 µL of Lipofectamine 3000 Transfection Reagent (Thermo Fisher Scientific) per well. Cells were assayed after 24 h post-transfection.

Co-Immunoprecipitation

MiaPaCa-2 cells, expressing GFP-NUPR1, were plated in 10 cm^2 dishes. When reached 80% confluence were treated with either 1 µM of Thapsigargin or glucose starved for 24 h. After that time cells were lysed on ice by using HEPES based lysis buffer containing proteases inhibitor cocktail (1:200) (Sigma P8340). Lysates were cleared for 10 min at 14000 rpm at 4°C and protein concentration of the supernatant was determined by using Protein Assay (BioRad). The co-immunoprecipitation was performed using GFP trap ® beads (chromotek) following manufacturer's protocol. The immunoprecipitates were pelleted, washed, denatured and blotted against eIF2α, p-eIF2α and anti GFP.

Click chemistry and fluorescence detection

Panc-1 and modified Panc-1 cells were grown on glass coverslips in DMEM supplemented with 10% bovine calf serum. After incubation for 3h or 6h with Thapsigargin, O-propargyl puromycin (OP-puro) was added to cells in complete culture medium for 1h. Cells were next washed with PBS and then fixed with 4% PFA in PBS. After fixation cells were permeabilized with 0.3% Triton-X in PBS. After the removal of detergent by PBS washes, CuAAC detection of OP-puro incorporated into nascent protein was performed by reacting the fixed cells for 1 h at room temperature with 20 µM FITC azide, as previously described (39). After staining, the coverslips were washed several times with TBST, counterstained with Hoechst, and mounted in standard mounting media. The stained cells were imaged by LSM 510 META confocal microscope (Zeiss) and on a Nikon Eclipse 90i fluorescence microscope. Stained cells were also quantified by Flow-cytometry in a MACSQuant-VYB (Miltenyi Biotec, Surrey, UK). Data analysis was carried out by using the FlowJo software.

Quantification of OP-Puro Labeling

The intensity of the fluorescent OP-puro stain in single cells was quantified by imageJ. Statistical significance was calculated by using two-way ANOVA and corrected for Sidak s test.

Proximity ligation assay

MiaPaCa-2 transfected with Flag-NUPR1 were treated with Thapsigargin (1μM), or glucose starved. After the indicated time points cells were washed twice in PBS, fixed, washed twice again, permeabilized in PBS/0.1% Triton X-100, and saturated with blocking solution for 30 min before immune-staining with Duolink by using PLA Technology (Sigma-Aldrich) following the manufacturer's protocol. Slides were processed for *in situ* PLA by using sequentially the Duolink *in situ* Detection Reagents Green, Duolink In Situ PLA Probe Anti-Mouse MINUS, and Duolink In Situ PLA Probe Anti-Rabbit PLUS. The following antibodies were used: rabbit monoclonal eIF2α XP® (D7D3, from Cell Signaling Technology), rabbit monoclonal Phospho-eIF2α XP® (Ser51) (D9G8, from Cell Signaling Technology), mouse monoclonal antibody anti-FLAG M2 (from Sigma-Aldrich). In these experiments, green fluorescence corresponds to the PLA-positive signal, and it indicates that the two molecules belong to the same protein complex. Blue fluorescence corresponds to nuclei (so-called DAPI staining). Protein overexpression was used to obtain a clearer and better signal. Preparations were mounted using Prolong Gold antifade reagent (Invitrogen) and image acquisition was carried out on an LSM 510 META confocal microscope (Zeiss) and on a Nikon Eclipse 90i fluorescence microscope.

Flag-NUPR1 and GFP-NUPR1 Co-immunoprecipitation and Mass spectrometry

MiaPaCa-2 cells, expressing Flag-NUPR1, were plated in 10 cm^2 dishes. When MiaPaCa-2 cells expressing Flag-NUPR1 or GFP-NUPR1 reached 60% confluence were lysed on ice by using HEPES based lysis buffer containing 10 mM NEM (N-Ethylmaleimide (Sigma 04259) and a proteases inhibitor cocktail (1:200) (Sigma P8340). Lysates were centrifuged for 10 min at 14000 rpm at 4°C. Protein concentration of the supernatant was determined by using Protein Assay (BioRad), and equal amounts of total protein were used to incubate with 30 μl of anti-Flag M2 coated beads under rotation for 2h at 4°C. Beads were then washed three times with cold lysis buffer and proteins were eluted using 250 μl ammonium hydrogen carbonate buffer containing 0.1 μg/μl of Flag peptide for 90 min while rotating at 4°C. After a short spin, the supernatant was recovered by using a Hamilton syringe. Protein samples were then concentrated by using Amicon Ultra-0.5 centrifugal filter devices (Millipore) according to manufacturer's instructions. Eluted proteins were collected and analyzed by mass spectrometry.

Mass Spectrometry Analysis

Protein extracts were loaded on NuPAGE 4-12% Bis-Tris acrylamide gels according to the manufacturer's instructions (Invitrogen). Running was stopped as soon as proteins stacked in a single band. Protein-containing bands were stained with Imperial Blue (Pierce), cut from the gel, and digested with high-sequencing-grade trypsin (Promega, Madison, WI) before mass spectrometry analysis as previously described. (40). Mass spectrometry analysis was carried out by LC−MS/MS using an LTQ-Velos-Orbitrap or a Q Exactive Plus Hybrid Quadrupole-Orbitrap (Thermo Electron, Bremen, Germany) online with a nanoLC Ultimate3000RSLC chromatography system (Dionex, Sunnyvale, CA). Five microliters corresponding to 1/5 of the whole sample were injected in triplicate on the system. After sample preconcentration and washing on a Dionex Acclaim PepMap 100 C18 column (2 cm x 100 µm i.d. 100 Å, 5 µm particle size), peptides were separated on a Dionex Acclaim PepMap RSLC C18 column (15 cm x 75 µm i.d., 100 Å, 2 µm particle size) at a flow rate of 300 nL/min, a two-step linear gradient (4-20% acetonitrile/H_2O; 0.1% formic acid for 90 min and 20-45% acetonitrile/H_2O; 0.1% formic acid for 30 min). For peptides ionization in the nanospray source, voltage was set at 1.9 kV and the capillary temperature at 275°C. All samples were measured in a data-dependent acquisition mode. Each experiment was preceded by a blank run to monitor system background. The peptide masses were measured in the LTQ-velos-orbitrap in a survey full scan (scan range 300-1700 m/z, with 30 K FWHM resolution at m/z = 400, target AGC value of 1.00 x 10^6, and maximum injection time of 200 ms). In parallel to the high-resolution full scan in the Orbitrap, the data dependent CID scans of the 10 most intense precursor ions were fragmented and measured in the linear ion trap (normalized collision energy of 35%, activation time of 10 ms, target AGC value of 1 x 10^4, maximum injection time 100 ms, and isolation window 2 Da). Parent masses obtained in Orbitrap analyzer were automatically calibrated on 445.1200 locked mass. Dynamic exclusion was implemented with a repeat count of 1 and exclusion time of 30 s. In the Q Exactive Plus Hybrid Quadrupole-Orbitrap, the peptide masses were measured in a survey full scan (scan range 375-1500 m/z, with 70 K FWHM resolution at m/z=400, target AGC value of 3.00 x 10^6 and maximum injection time of 100 ms). Following the high-resolution full scan in the Orbitrap, the 10 most intense data-dependent precursor ions were successively fragmented in higher energy collisional dissociation (HCD) cell and measured in Orbitrap (normalized collision energy of 25%, activation time of 10 ms, target AGC value of 1.00 x 10^3, intensity threshold 1.00 x 10^4 maximum injection time 100 ms, isolation window 2 m/z, 17.5 K FWHM resolution, scan range 200 to 2000 m/z). Dynamic exclusion was implemented with a repeat count of 1 and exclusion time of 20 s.

Mass Spectrometry Data Analysis

Raw files generated from mass spectrometry analysis were processed using Proteome Discoverer 1.4.1.14 (Thermo Fisher Scientific). This software was used to search data *via* in-house Mascot server (version 2.3.0; Matrix Science, London, U.K.) against the Human database subset of the SwissProt database (version 2017.03, 20184 human entries). A database search was done by using the following settings: a maximum of two trypsin miscleavage allowed, methionine oxidation and protein N-acetylation as dynamic modifications, and cysteine carbamido-methylation as fixed modification. A peptide mass tolerance of 6 ppm and a fragment mass tolerance of 0.8 Da were allowed for search analysis. Only peptides identified with a FDR < 1% were used for protein identification.

Acknowledgements

The work was supported by La ligue Contre le Cancer, INCa, Canceropole PACA and INSERM. The electron microscopy experiments were performed in the PiCSL-FBI core facility (IBDM, AMU-Marseille). The confocal microscopy experiments were performed in the “Plateforme de Microscopie et Imagerie Scientifique” of CRCM of Marseille.

References

1. G. V. Mallo, *et al.*, Cloning and expression of the rat p8 cDNA, a new gene activated in pancreas during the acute phase of pancreatitis, pancreatic development, and regeneration, and which promotes cellular growth. *J. Biol. Chem.* **272** (1997).
2. D. Grasso, *et al.*, Genetic inactivation of the pancreatitis-inducible gene Nupr1 impairs PanIN formation by modulating Kras G12D-induced senescence. *Cell Death Differ.* **21**, 1633 (2014).
3. M. R. Emma, *et al.*, NUPR1, a new target in liver cancer: implication in controlling cell growth, migration, invasion and sorafenib resistance. *Cell Death Dis.* **7**, e2269 (2016).
4. V. Giroux, *et al.*, p8 is a new target of gemcitabine in pancreatic cancer cells. *Clin. cancer Res.* **12**, 235–241 (2006).
5. T. Hamidi, *et al.*, Nupr1-Aurora Kinase A Pathway Provides Protection against Metabolic Stress-Mediated Autophagic-Associated Cell Death. *Clin. Cancer Res.* **18**, 5234 LP – 5246 (2012).
6. J. Averous, *et al.*, Amino acid deprivation regulates the stress-inducible gene p8 via the GCN2/ATF4 pathway. *Biochem. Biophys. Res. Commun.* **413**, 24–29 (2011).
7. A. Garcia-Montero, *et al.*, Expression of the stress-induced p8 mRNA is transiently activated after culture medium change. *Eur. J. Cell Biol.* **80** (2001).
8. H. C. Barbosa-Sampaio, *et al.*, Nupr1 deletion protects against glucose intolerance by increasing beta cell mass. *Diabetologia* **56**, 2477–2486 (2013).
9. T. Hamidi, *et al.*, NUPR1 works against the metabolic stress-induced autophagy-associated cell death in pancreatic cancer cells. *Autophagy* **9**, 95–97 (2013).
10. D. W. Clark, *et al.*, NUPR1 interacts with p53, transcriptionally regulates p21 and rescues breast epithelial cells from doxorubicin-induced genotoxic stress. *Curr. Cancer Drug Targets* **8**, 421–430 (2008).
11. D. Taïeb, *et al.*, Inactivation of stress protein p8 increases murine carbon tetrachloride hepatotoxicity via preserved CYP2E1 activity. *Hepatology* **42**, 176–182 (2005).
12. A. H. Schönthal, Endoplasmic reticulum stress: its role in disease and novel prospects for therapy. *Scientifica (Cairo).* **2012**, 857516 (2012).
13. C. H. Kubisch, C. D. Logsdon, Endoplasmic reticulum stress and the pancreatic acinar cell. *Expert Rev. Gastroenterol. Hepatol.* **2**, 249–260 (2008).
14. D. Ron, P. Walter, Signal integration in the endoplasmic reticulum unfolded protein response. *Nat. Rev. Mol. cell Biol.* **8**, 519 (2007).
15. J. E. Chambers, *et al.*, Actin dynamics tune the integrated stress response by regulating eukaryotic initiation factor 2α dephosphorylation. *Elife* **4**, e04872 (2015).
16. M. Livezey, R. Huang, P. J. Hergenrother, D. J. Shapiro, Strong and sustained

activation of the anticipatory unfolded protein response induces necrotic cell death. *Cell Death Differ.* **25**, 1796–1807 (2018).

17. H. Kato, H. Nishitoh, Stress responses from the endoplasmic reticulum in cancer. *Front. Oncol.* **5**, 93 (2015).
18. P. Santofimia-Castaño, *et al.*, Inactivation of NUPR1 promotes cell death by coupling ER-stress responses with necrosis. *Sci. Rep.* **8**, 16999 (2018).
19. D. Cai, *et al.*, Nupr1/Chop signal axis is involved in mitochondrion-related endothelial cell apoptosis induced by methamphetamine. *Cell Death Dis.* **7**, e2161–e2161 (2016).
20. H. Jin, *et al.*, Nuclear protein 1 induced by ATF4 in response to various stressors acts as a positive regulator on the transcriptional activation of ATF4. *IUBMB Life* **61**, 1153–1158 (2009).
21. M. Calfon, *et al.*, IRE1 couples endoplasmic reticulum load to secretory capacity by processing the XBP-1 mRNA. *Nature* **415**, 92–96 (2002).
22. E. Malzer, *et al.*, The integrated stress response regulates BMP signalling through effects on translation. *BMC Biol.* **16**, 34 (2018).
23. H. P. Harding, *et al.*, An integrated stress response regulates amino acid metabolism and resistance to oxidative stress. *Mol. Cell* **11**, 619–633 (2003).
24. S. J. Marciniak, *et al.*, CHOP induces death by promoting protein synthesis and oxidation in the stressed endoplasmic reticulum. *Genes Dev.* **18**, 3066–3077 (2004).
25. R. Kramer, *et al.*, Inhibition of N-linked glycosylation of P-glycoprotein by tunicamycin results in a reduced multidrug resistance phenotype. *Br. J. Cancer* **71**, 670 (1995).
26. D. W. Reid, Q. Chen, A. S.-L. Tay, S. Shenolikar, C. V Nicchitta, The unfolded protein response triggers selective mRNA release from the endoplasmic reticulum. *Cell* **158**, 1362–1374 (2014).
27. D. Sicari, A. Delaunay-Moisan, L. Combettes, E. Chevet, A. Igbaria, A guide to assessing endoplasmic reticulum homeostasis and stress in mammalian systems. *FEBS J.* (2019).
28. S. Schuck, W. A. Prinz, K. S. Thorn, C. Voss, P. Walter, Membrane expansion alleviates endoplasmic reticulum stress independently of the unfolded protein response. *J. Cell Biol.* **187**, 525–536 (2009).
29. P. Santofimia-Castaño, *et al.*, Ligand-based design identifies a potent NUPR1 inhibitor exerting anticancer activity via necroptosis. *J. Clin. Invest.* **129**, 2500–2513 (2019).
30. J. Han, *et al.*, ER-stress-induced transcriptional regulation increases protein synthesis leading to cell death. *Nat. Cell Biol.* **15**, 481 (2013).
31. J. Mayerle, M. Sendler, M. M. Lerch, Secretagogue (Caerulein) induced pancreatitis in rodents. *Pancreapedia Exocrine Pancreas Knowl. Base* (2013).

32. U. R. Chowdhury, R. S. Samant, O. Fodstad, L. A. Shevde, Emerging role of nuclear protein 1 (NUPR1) in cancer biology. *Cancer Metastasis Rev.* **28**, 225–232 (2009).
33. D. Scheuner, *et al.*, Translational control is required for the unfolded protein response and in vivo glucose homeostasis. *Mol. Cell* **7**, 1165–1176 (2001).
34. C. Wójcik, *et al.*, Valosin-containing protein (p97) is a regulator of endoplasmic reticulum stress and of the degradation of N-end rule and ubiquitin-fusion degradation pathway substrates in mammalian cells. *Mol. Biol. Cell* **17**, 4606–4618 (2006).
35. H. P. Harding, Y. Zhang, D. Ron, Protein translation and folding are coupled by an endoplasmic-reticulum-resident kinase. *Nature* **397**, 271 (1999).
36. W.-X. Ding, *et al.*, Differential effects of endoplasmic reticulum stress-induced autophagy on cell survival. *J. Biol. Chem.* **282**, 4702–4710 (2007).
37. S. Vasseur, *et al.*, p8-deficient fibroblasts grow more rapidly and are more resistant to adriamycin-induced apoptosis. *Oncogene* **21**, 1685 (2002).
38. J. M. Chirgwin, A. E. Przybyla, R. J. MacDonald, W. J. Rutter, Isolation of biologically active ribonucleic acid from sources enriched in ribonuclease. *Biochemistry* **18**, 5294–5299 (1979).
39. A. Salic, T. J. Mitchison, A chemical method for fast and sensitive detection of DNA synthesis in vivo. *Proc. Natl. Acad. Sci.* **105**, 2415–2420 (2008).
40. A. Snevechenko, M. Wilm, O. Vorm, M. Mann, Mass spectrometric sequencing of proteins silver-stained polyacrilamide gels. *Anal. Chem.* **68**, 850–858 (1996).